INITIAL DESIGN OF A LUMPED INDUCTANCE KICKER FOR THE FCC-EE

G. Sergentanis*, L. Ducimetière, Y. Dutheil, S. Dylan, G. Favia, T. Kramer, J. Ruf, S. Yue
European Organization for Nuclear Research, Geneva, Switzerland

Abstract

CERN is working towards a new, larger circular collider complex, the Future Circular Collider (FCC-ee), with a perimeter of 90.7 km. This paper addresses some of the challenges associated with beam-transfer equipment. The FCC-ee requires numerous kicker systems for beam disposal and transfers from injectors to the main collider ring. To standardise hardware parameters across machines and reduce the variety of beam-line components, this work proposes a lumped-inductance kicker magnet for multiple systems. To adapt the design for different purposes within the FCC complex, only the number of modules is adjusted to achieve the required deflection, while maintaining a low voltage for each module to enable operation outside the vacuum. This common design offers significant advantages for spares, maintenance, production, and machine protection. Initial design-study results from numerical simulations of the beam-line element are presented, along with system-level options for integration with the FCC-ee accelerator.

INTRODUCTION

The FCC-ee, a proposal for CERN's next flagship accelerator, will enable higher precision measurements of the Higgs particle with collision energies up to 365 GeV in the $t\bar{t}$ mode [1].

Key accelerator systems are currently being developed as part of the project's reference design phase. These include the injection and extraction systems, which comprise kicker magnets to steer the beam. Established kicker technologies comprise lumped inductance, transmission line, and stripline kickers, with the selection depending on required beam timings, desired deflection angles, and available beamline length [2].

Lumped Inductance (LI) kickers offer strong beam deflection capabilities and are cost-effective due to their simplicity and robustness. A primary limitation is that achieving field rise and fall times considerably below the 1 µs range is challenging, given their lumped-element nature and the travelling wave phenomena in cable connections [2]. The injection and extraction kicker systems for the FCC-ee and their requirements have been outlined in [3]. Table 1 details the systems for which an LI kicker magnet topology has been chosen, along with their key specifications. This paper presents the design of a common LI kicker magnet module suitable for all these systems. While the requirements for the magnetic field homogeneity are identical for these systems, the necessary deflection angle (kick strength) varies. These differing requirements can be accommodated by using a variable number of identical modules based on a single LI kicker design, as well as by varying their generator characteristic impedance.

Table 1: FCC-ee LI Kicker System Requirements

	Booster extraction	**Booster dump**	**Collider injection**	**Collider dump**
Energy [GeV]	45–182.5	45–182.5	45–182.5	45–182.5
Kick angle [mrad]	0.196	0.396	0.08	0.396
Rise/fall times [ns]	600	600	600	600
Flat top length [µs]	304	304	304	304
Flat top quality [%]	±0.6	±20	±1.5	±20
Maximum repetition rate [Hz]	0.3	1	0.3	0.1
Magnetic field homogeneity [%]	0.5	0.5	0.5	0.5

MAGNET DESIGN

The design of an appropriate LI kicker must satisfy several key requirements. The magnetic field quality must meet the specifications set by beam optics considerations. Additionally, the inductance must be sufficiently low to enable the required magnetic field rise and fall times. Other important considerations include the beam-coupling impedance and its impact on beam stability.

Field Quality

One of the challenges in the magnet design is the required magnetic field homogeneity of ±0.5%. The field homogeneity is defined as the maximum deviation of the vertical magnetic field within the good field region (GFR) compared to its centre point value. For this design, the GFR is preliminary defined to coincide with the required beam stay-clear area (BSC). This deviation is calculated as shown in Eq. (1), with the y-axis being the vertical axis of the magnet cross section.

$$\Delta B_y = \left| \frac{B_y - B_{y,\text{centre}}}{B_{y,\text{centre}}} \right| \cdot 100\% \tag{1}$$

An initial design choice is the shape of the magnetic yoke, with options including a C-core and a window-frame topology. A window-frame magnet fully encloses the busbars with ferrite material, splitting the magnetic flux between two return paths and allowing the use of a thinner yoke for the same magnetic field strength and aperture. Furthermore, its symmetric field distribution, makes the window-frame design more suitable for meeting the stringent field homogeneity requirements.

* grigorios.sergentanis@cern.ch

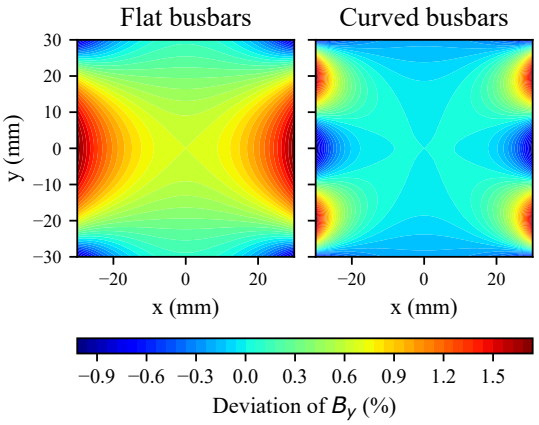

Figure 1: Field homogeneity with flat and shaped busbars.

Finally, the design foresees the insertion of an alumina chamber, which houses the vacuum and serves as a mechanical support for a beam screen.

Static Behaviour

Design studies have been conducted using ANSYS Maxwell [4]. To establish a baseline, the field homogeneity was first evaluated under magneto-static conditions, assuming a uniform current density across the conductor cross-section. An initial simulation of a window-frame magnet accommodating a large 60 mm by 60 mm square BSC, based on the FCC-ee beam pipe diameter, was performed to assess the achievable field homogeneity. The conductor features a 5 mm horizontal thickness and is surrounded by a 2.5 mm insulation clearance. The distance between the busbars is 81 mm, and the vertical aperture is 76 mm, selected to accommodate an alumina chamber, including mechanical tolerances. As shown in Fig. 1 (left), the resulting field homogeneity for flat conductors falls outside the acceptable range across most of the horizontal aperture. To mitigate this, the conductor profile was optimised by adding bumps near the corners of the GFR. This modification yielded the significantly improved homogeneity depicted in Fig. 1 (right). This design aperture was based on preliminary GFR estimates. Following this evaluation, a highly flat beam profile was established by the beam optics, allowing for a reduced and, consequently, more efficient vertical aperture for the subsequent design stages.

Transient Behaviour

Transient 2D field simulations showed that the current density distribution in the conductors shifts over the 304 µs pulse duration, due to skin and proximity effects. The observed behaviour is consistent with established literature on magnetic field diffusion in conductive slabs [5]. Consequently, for 5 mm copper conductors, a steady state current distribution is not reached within the pulse time frame, making transient studies more suitable for the magnet design.

In addition to the dynamics caused by magnetic diffusion, the transient current distribution is heavily governed by the

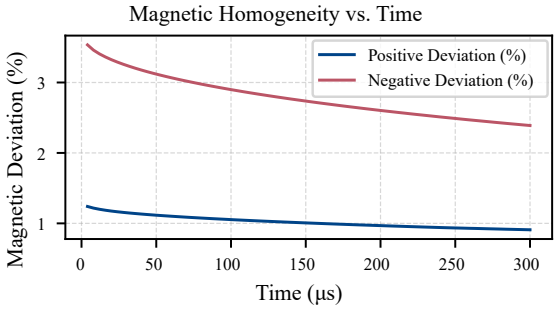

Figure 2: Field homogeneity with curved windings in the time-domain.

proximity effect. During the fast transients of the excitation pulse, the current concentrates along paths of minimal impedance to reduce the system's overall inductance. The previously introduced bumps on the copper busbars exacerbate these dynamics by providing localised low-impedance paths. As a result, pronounced current crowding occurs at these specific locations, causing the magnetic field homogeneity to remain highly dynamic and outside the allowed specifications (Table 1) for much of the pulse duration. This degraded transient field quality is illustrated in Fig. 2.

Extensive investigations were conducted to develop a magnetic design that maintains the required field homogeneity throughout the 304 µs pulse duration. Simultaneously, the vertical aperture was reduced to minimise the stored energy, thereby relaxing the requirements for the pulsed power generator. Incorporating input from beam physics and mechanical considerations, the resulting magnet cross-section is shown in Fig. 3, featuring a vertical aperture of 30 mm. In this figure, the preliminary beam chamber cross section is shown in black, while the light green rectangle highlights the area considered for field homogeneity evaluation, designated as the GFR, measuring 60 × 4 mm in the full model. The model includes a eddy-current shield, located between two ferrites halves and intended to shield the magnetic field induced by the beam in the yoke. Due to the computational demands of time-domain solvers, quarter-symmetry conditions were applied to accelerate simulations. Consequently, the subsequent results represent a quarter of the full magnet geometry.

With a flat conductor profile, the magnetic field distribution did not meet the required field homogeneity specifications. To address this, a gap was introduced, effectively splitting each conductor into two parallel sections. To improve manufacturability, this parallel arrangement was approximated by a single grooved conductor. By ensuring a sufficient groove depth, the current flowing through the connecting bridge remains negligible over the duration of the pulse. This solution is termed 'quasi-parallel' LI kicker. Optimisation of the geometry for transient field homogeneity yielded the cross-section shown in Fig. 3, which features a 7 mm wide and 2.5 mm deep groove. The total horizontal copper thickness remains 5 mm, and a 2.5 mm clearance surrounding the conductor is preserved for electrical insulation and mechanical tolerances.

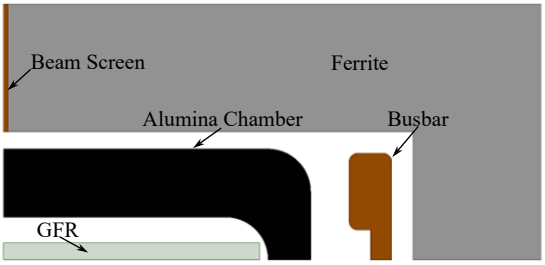

Figure 3: Quarter-Symmetric 2D 'quasi-parallel' kicker model.

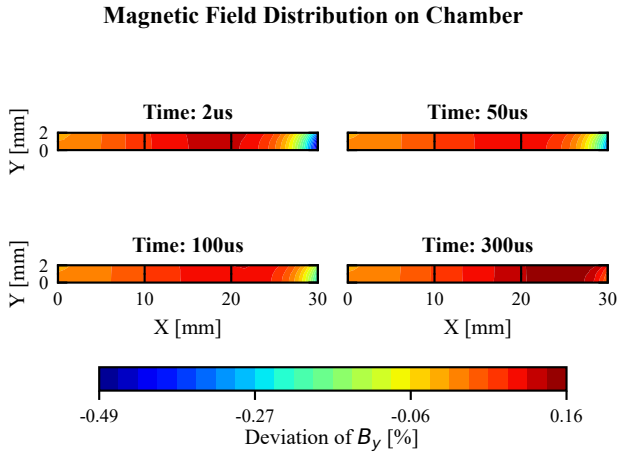

Figure 4: Field homogeneity with the 'quasi-parallel' windings in the time-domain.

A transient analysis was performed with this geometric configuration to verify compliance with the required specifications. The model is driven by a trapezoidal current excitation featuring a 600 ns rise and fall time and a 304 µs flattop. The simulated field homogeneity for four time steps along the pulse flat-top is shown in Fig. 4. The field homogeneity meets the required specification at the beginning of the flattop and improves as the pulse progresses.

A conductive beam chamber coating is foreseen to minimise beam coupling impedance and reduce beam-induced heating. However, eddy currents induced in this coating will partially shield the fast-rising magnetic field, negatively impacting both the field rise time and homogeneity. Consequently, the coating thickness must be determined as a compromise: it must be sufficiently thick to carry the beam image current, yet thin enough to limit degradation of the kicker magnet's transient performance.

SYSTEM-LEVEL REQUIREMENTS

With the cross-sectional magnet geometry established in the preceding sections, the total magnet length per kicker system is driven by the integrated field necessary to achieve the specified deflection. Conversely, the length of each individual magnet module is constrained by the rise time requirements, as a longer module possesses a larger inductance. Therefore, a chain of multiple identical magnet modules is foreseen for each system. These fundamental dependencies are described by Eqs. (2)–(5).

$$B\rho \approx 3.3356 \cdot E(\mathrm{GeV}) \quad (2) \qquad \theta_{\mathrm{def}} = \frac{\int B\,dl}{B\rho} \quad (3)$$

$$L_{\mathrm{kicker}} \approx \mu_0 \cdot \frac{H_{\mathrm{ap}}}{V_{\mathrm{ap}}} \cdot l \quad (4) \qquad t_{\mathrm{rise}} \approx 5 \cdot \frac{L_{\mathrm{kicker}}}{Z_{\mathrm{system}}} \quad (5)$$

Equations (2) and (3) describe the beam rigidity for ultra-relativistic particles and the resulting deflection angle from an integrated magnetic field. The inductance of the kicker module is determined by its magnetic aperture and physical length, as defined by Eq. (4). Consequently, this inductance, combined with the characteristic system impedance, estimates the achievable field rise time as shown in Eq. (5). A higher system impedance yields a faster current rise time, but requires a correspondingly higher driving voltage to achieve the necessary magnet current.

Assuming an initial baseline system impedance of 10 Ω, Table 2 summarises the expected minimal number of magnets for each FCC-ee kicker system. To facilitate a straightforward pulse generator design and reliable magnet insulation for out-of-vacuum operation, the driving voltage and nominal current were limited to 10 kV and 1 kA, respectively. For certain systems, pending machine protection considerations may prescribe a higher minimum number of magnet modules. Furthermore, the low-pass shielding effect of the beam chamber coating may necessitate for additional margin in the current rise time to compensate for the delayed field penetration, which may make a higher system impedance more suitable. Finally, the total number of magnets will likely increase in the final design to account for the availability of hot spare LI kicker modules.

Table 2: Summary of System Parameters

System	Expected Field [mT]	Max. Magnet Length [m]	Min. No. of Magnets
Booster Extraction	41.89	0.347	9
Collider Injection	41.89	0.347	4
Collider Dump	41.89	0.347	17
Booster Dump	41.89	0.347	17

CONCLUSION

A common lumped-inductance kicker magnet module design has been proposed to serve multiple injection and extraction systems across the FCC-ee complex. An optimum coil geometry has been developed, to mitigate dynamic proximity effects while meeting the stringent ±0.5% field homogeneity requirements over the entire 304 µs flattop. System-level calculations show that adjusting the number of modules enables the various deflection requirements to be met while keeping the operational voltage and current within acceptable limits. With no major showstoppers identified so far, future work will focus on 3D electromagnetic modelling, beam coupling impedance studies, including the beam chamber coating, pulse generator design, and final system impedance optimisation.

REFERENCES

[1] P. Janot and C. Grojean, 'FCC: the physics case', *CERN Courier*, vol. 64, no. 2, pp. 21–24, Mar. 2024. https://cerncourier.com/a/fcc-the-physics-case/

[2] M. Barnes, 'Kicker systems', *CERN Yellow Rep. School Proc.*, vol. 5, p. 229, 2018. doi:10.23730/CYRSP-2018-005.229

[3] T. Kramer *et al.*, 'Feasibility of kicker systems for FCC-ee and injectors', in *Proc. IPAC'25*, Taipei, Taiwan, pp. 470–473, Nov. 2025. doi:10.18429/JACoW-IPAC2025-MOPM065

[4] ANSYS, Inc., 'ANSYS Maxwell', Electromagnetic field simulation software, 2024, https://www.ansys.com/products/electronics/ansys-maxwell,

[5] S. Russenschuck, 'Field diffusion', in *Field Simulation for Accelerator Magnets*. John Wiley & Sons, Ltd, 2025, pp. 319–338. doi:10.1002/9783527839599.ch8